IEEE/CSC & ESAS SUPERCONDUCTIVITY NEWS FORUM (global edition), January 2017 (Preview 1).
Preprint of ASC 2016 manuscript 2EPo2D-08 submitted to *IEEE Trans. Appl. Supercond.* for possible publication.
DOI: 10.1109/TASC.2016.2631427

High-Inductance Bi-SQUID

Victor. K. Kornev, *Member, IEEE*, Nikolay V. Kolotinskiy, *Member, IEEE*, Daniil E. Bazulin, and Oleg A. Mukhanov, *Fellow, IEEE*

***Abstract*—We performed an in-depth numerical analysis of high inductance bi-SQUIDs with normalized inductance of its one-junction loop $l >> 1$. This is desired for better coupling with the external signals and for the high temperature superconductor implementations. Typically the high linearity (up to 90 dB) can be achieved in bi-SQUIDs at $l \leq 1$ at which its flux-to–voltage characteristic has a distinct triangular shape. We showed that the high linearity can be also achieved at $l > 1$, when bi-SQUID has a hysteretic response. The critical current of the third Josephson junction is to be of the same order as the one of the other two Josephson junctions, and inductance l_{DC} of the second (two-junction) loop is allowed to be as high as about $l/4$ in the presence of the high linearity.**

***Index Terms*—Josephson junctions; bi-SQUID; highly linear voltage output; high inductance; hysteretic mode.**

I. Introduction

Bi-SQUID was introduced [1] to improve the linearity of the flux-to-voltage transformation of dc SQUIDs. The higher linearity of bi-SQUIDs allows extending their applications to high-frequency signals [2]-[4], when an external feedback loop commonly used for linearization of dc SQUID response is no longer feasible. As shown schematically in Fig. 1, bi-SQUID contains two conjugated loops, an rf SQUID loop and a dc SQUID loop, providing flux-to-phase and phase-to-voltage signal transformations, respectively. The nonlinear behavior of these two transformations can be set mutually inverse, resulting in a triangular and, therefore, highly linear voltage response to the applied magnetic flux. According to the approximate analytical analysis, when considering inductance L_{DC} of the dc SQUID loop negligibly small [1], this can be achieved at $l^* = l \cdot i_{c3} \sim 1$, where $l = 2\pi I_C L_{RF}/\Phi_0$ is normalized inductance of the rf SQUID loop, $i_{c3} = I_{c3}/I_C$ is normalized *c*ritical current of the third junction (in rf SQUID loop) with $I_C = I_{c1} = I_{c2}$. This simplified theory neglects the pulse component of the J1-J2 junctions' phase difference $\varphi_1 - \varphi_2 = \varphi_3$ (Fig. 1). Moreover, the phase-to-voltage transformation is accounted as the one provided by a zero-inductance dc SQUID. These assumptions are accurate only in the case of very small inductance $l << 1$. For other cases, a numerical simulation has to be used for circuit analysis. In spite of many publications reporting numerical simulations of bi-SQUIDs and arrays of bi-SQUIDs [5]-[11], the attainability of the high-linearity voltage output at high inductance of the rf SQUID loop is still obscure, while examples of the linear triangular responses were always demonstrated at $l \sim 1$ only.

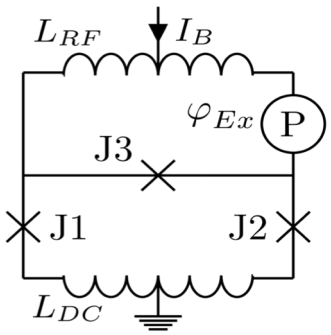

Fig. 1. Bi-SQUID equivalent circuit with L_{RF} - inductance of rf SQUID loop and L_{DC} - inductance of dc SQUID loop. The phase source 'P' of φ_{ex} describes an external magnetic flux $\Phi_{ex} = \varphi_{ex}\Phi_0/2\pi$ applied to the rf SQUID loop.

However for practical considerations, the increase in the loop inductance is desired for better coupling with an input circuit. The large loop inductance is also inevitable in the case of a single-layer implementation when ground plane layer is not available, most notably for High Temperature Superconductor (HTS) fabrication process (e. g., [11]-[14]). In this paper, we consider how to attain the highly linear flux-to-voltage conversion for bi-SQUIDs with large inductance. The study is performed in the frame of a current-biased mode of bi-SQUID [15] and standard Resistively Shunted Josephson-junction (RSJ) model [16] with negligibly small capacitance.

II. Pulse Component Impact

In bi-SQUIDs, both the flux-to-phase and phase-to-voltage transformations differ from the ones characteristic for a stand-alone rf SQUID or dc SQUID, respectively. The difference is caused by the nonlinear interaction of these loops with involvement of the pulse component $\widetilde{\varphi_3}$, appearing in the 3-rd junction phase φ_3 under Josephson oscillation process in the

Manuscript received September 6, 2016.

V.K. Kornev, N.V. Kolotinskiy, D.E. Bazulin are with Department of Physics, Lomonosov Moscow State University, 119991, Moscow, Russia. (e-mail: kolotinskij@physics.msu.ru).

O. A. Mukhanov is with Hypres, Inc., 175 Clearbrook Road, Elmsford, NY 10523, USA. (e-mail: mukhanov@hypres.com).

IEEE/CSC & ESAS SUPERCONDUCTIVITY NEWS FORUM (global edition), January 2017 (Preview 1).
Preprint of ASC 2016 manuscript 2EPo2D-08 submitted to *IEEE Trans. Appl. Supercond.* for possible publication.
DOI: 10.1109/TASC.2016.2631427

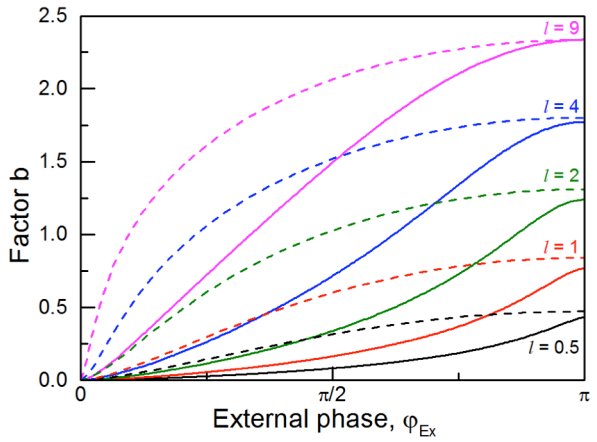

Fig. 2. Factor b versus input phase φ_{ex} at different inductances l = 0.5, 1, 2, 4, 9 for single dc SQUID (dashed lines) and bi-SQUID with l^*= 1 (solid lines).

dc SQUID loop (at dc biasing $I_b > 2I_C$). In fact, the periodic transient of the single flux quanta through this loop generates an ac circular current which imposes the pulse phase drop $\widetilde{\varphi_3}$ on the junction J3. The signal (low frequency) component $\overline{\varphi_3}$ of the junction phase $\varphi_3 = \overline{\varphi_3} + \widetilde{\varphi_3}$ controls the nonlinear impedance of the junction and hence the form and amplitude of the circular current. Thereby it affects the phase-to-voltage transformation due to a self-detection effect.

In turn, as derived in [17], the input magnetic flux $\Phi_{ex} = 2\pi\varphi_{ex}/\Phi_0$ is transformed into the signal component $\overline{\varphi_3}$ in compliance with the 'phase' equation

$$\overline{\varphi_3} = \varphi_{ex} - l_{eff}\sin(\overline{\varphi_3}), \quad (1)$$

which is of conventional form but operating with the pulse-phase-dependent effective inductance

$$l_{eff} = l^* \cdot J_0(b_1)J_0(b_2)J_0(b_3)\ldots, \quad (2)$$

where b_1, b_2, b_3, … are the amplitudes of the harmonic expansion for the pulse component of the phase difference, and $J_0(.)$ is the 0-th order Bessel function of the first kind. When the amplitudes are small enough, the Bessel function can be approximated by a serial expansion to a second term, and hence the effective inductance can be written as follows:

$$l_{eff} \approx l^* \cdot (1 - b^2/4), \quad (3)$$

$$b^2 = b_1^2 + b_2^2 + b_3^2 + \cdots. \quad (4)$$

Fig. 2 shows the factor b calculated numerically (see details in [8]) versus input phase φ_{ex} at different inductances l for single dc SQUID and bi-SQUID with l^*= 1. In both devices, the pulse phase component increases with the input magnetic flux and inductance l while remaining always less in bi-SQUID.

III. Triangular Voltage Response

At small inductances $l \leq 1$, when the factor b is quite small, an influence of the small pulse phase component helps to make the flux-to-phase and phase-to-voltage transformations mutually inverse and thereby to attain the highly linear triangular voltage response. Fig. 3 shows the transformations which can be achieved at l = 0.2 when l^*= 0.4 (top) and at l = 1 when l^*= 1 (bottom). One can see that these curves are coincident in the range from 0 to some point close to π. In view of the π-point symmetry of the 2π-periodic voltage response, the coincidence implies mutual compensation of these flux-to-phase and phase-to-voltage transformations in the entire range except some small section near $\varphi_3 = \pi$. For reference, the ultimate voltage response $V/V_C = |\sin(\varphi_3/2)|$ of a single dc SQUID (when $\varphi_3 = \varphi_{ex}$) with negligibly small inductance is presented with dash lines. Insets show the resulting voltage responses. When exploiting up to 30% to 50% of the response swing, the linearity of the voltage outputs can be as high as 90 and 70 dB, respectively. The linearity analysis was performed numerically in accordance to the standard one-tone analysis technique as follows (see also [18], [19]). When applying a sinusoidal input signal, the device linearity is derived with formula $Lin = b_1/max\{b_k\}$, where b_1 and b_k are the amplitudes of basic tone and harmonic components of the output signal.

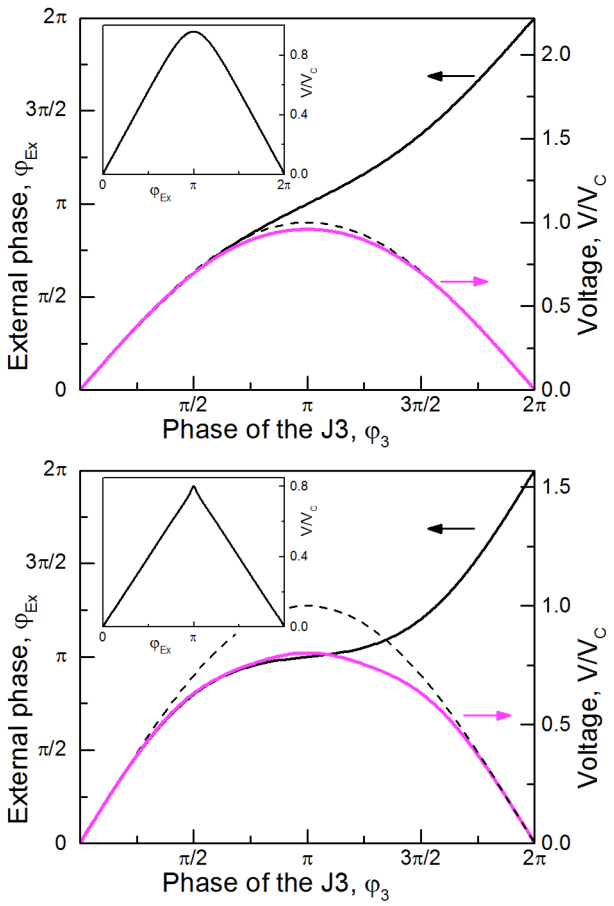

Fig. 3. The flux-to-phase transformation (black solid line) and the phase-to-voltage transformation (solid magenta line) at l = 0.2, l^* = 0.4 (*a*) and l = 1, l^* = 1 (*b*); both at I_B=2I_C The dashed lines show voltage response $V/V_C = |\sin(\varphi_3/2)|$ of a single dc SQUID with negligibly small inductance, when $\varphi_3 = \varphi_{ex}$, at the same current biasing I_B=2I_C. Insets show respective voltage responses of the bi-SQUIDs.

IEEE/CSC & ESAS SUPERCONDUCTIVITY NEWS FORUM (global edition), January 2017 (Preview 1).
Preprint of ASC 2016 manuscript 2EPo2D-08 submitted to *IEEE Trans. Appl. Supercond.* for possible publication.
DOI: 10.1109/TASC.2016.2631427

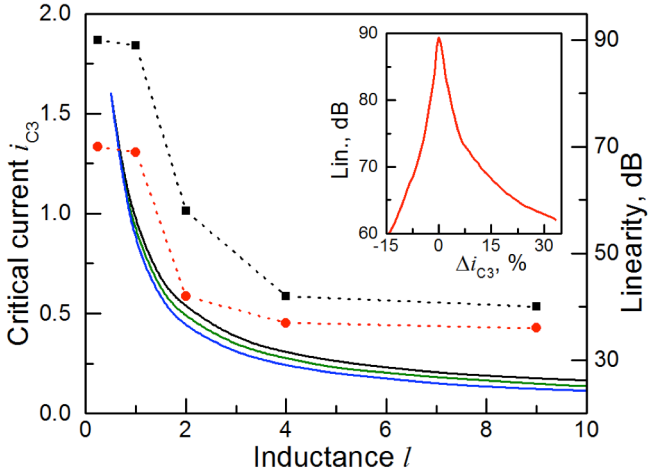

Fig. 4. Critical current i_{c3} as a function of the rf SQUID loop inductance l, when the bi-SQUID voltage response approaches triangular form, at the normalized value of the dc SQUID loop inductance l_{dc} = 0 (black line), l/2 (green line), l (blue line). The dashed lines show the reachable linearity as function of l when signal exploits 30% (black line with boxes) and 50% (red line with circles) of the total voltage response swing. Inset shows dependence of the response linearity at l = 1 (l_{dc} < 1/2) on departure of i_{c3} from its optimal value.

When pursuing the voltage response most closely approaching a triangular form in wide range of the inductances, Fig. 4 presents the critical current i_{c3} as function of the rf loop inductance l (solid lines) at different values of the dc SQUID loop inductance l_{dc} (up to l) and the reachable linearity (dash lines with symbols). Inset in Fig. 4 shows the response linearity at l = 1 versus departure of the critical current i_{c3} from its optimal value, when the signal exploits 30% of the total response swing. It is very important from a practical viewpoint that the attainable linearity remains about the same (with accuracy within 3 dB) with increase of l_{dc} up to about l/2, but the further increase of the inductance leads to a significant reduction of the attainable linearity. Such a high linearity achievable at $l \le 1$ cannot be achieved at $l > 1$. As it is evidenced in Fig. 4, the attainable response linearity rapidly decreases from 90 dB at l = 1 down to 40 dB at l = 4 and keeps decreasing with the inductance increasing. The underlying cause of this reduction is the increase of the pulse phase component upsetting the achieved mutual inverse of the flux-to-phase and phase-to-voltage transformations.

IV. Hysteretic Voltage Response

Our in-depth numerical analysis of the bi-SQUID characteristics has shown that the highly linear voltage output is attainable within wide range of the device inductances, but outside the domain of triangular response form when $l > 1$.

At high inductance $l > 1$, the pulse phase component $\widetilde{\varphi_3}$ can be restricted using a hysteretic mode of the bi-SQUID operation, when the range of the high pulse component existence $\pi/2 < \overline{\varphi_3} < 3\pi/2$ is cut off. In this mode, voltage response is hysteretic but showing substantially high linearity. Fig. 5 shows the high linearity voltage response (top) which is

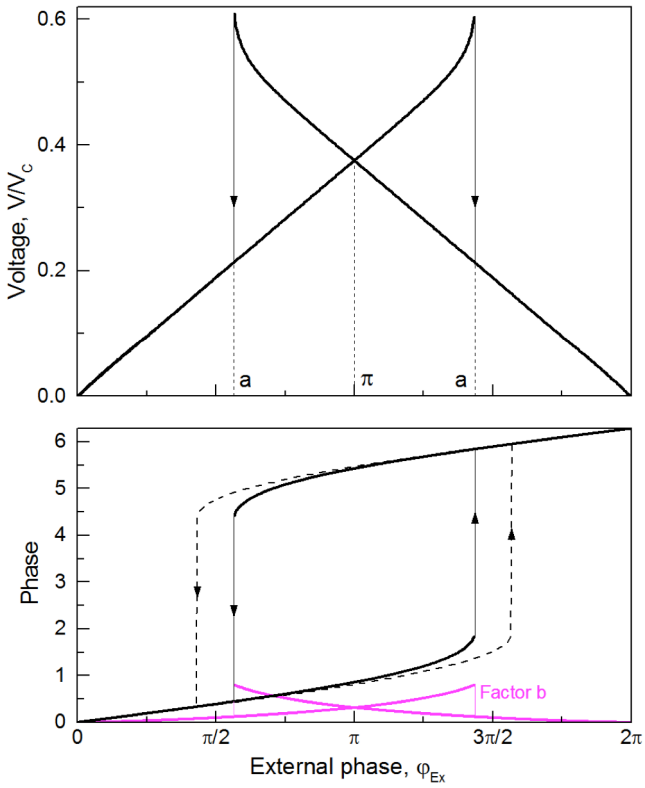

Fig. 5. The highly linear hysteretic voltage response of bi-SQUID at l = 4 and i_{c3} =0.8 when l^* = 3.2, as well as the corresponding flux-to-phase transformation (black solid line) and factor b (magenta line). Single rf SQUID with the same inductance $l = l^* = 3.2$ provides flux-to-phase transformation shown by the dashed line.

attainable at l = 4 when l^* = 3.2 (at i_{c3} = 0.8), as well as the corresponding flux-to-phase transformation and factor b characterizing amplitude of the pulse phase component (bottom). The existence of some small pulse component makes the effective hysteresis less than the one in the flux-phase relation of a single rf SQUID with the same inductance $l = l^* = 3.2$ (shown by dashed line). It is seen that the hysteretic flux-phase relation provides cutting off the phase $\overline{\varphi_3}$ values where the factor b could be excessively high and thereby could disturb the response linearity.

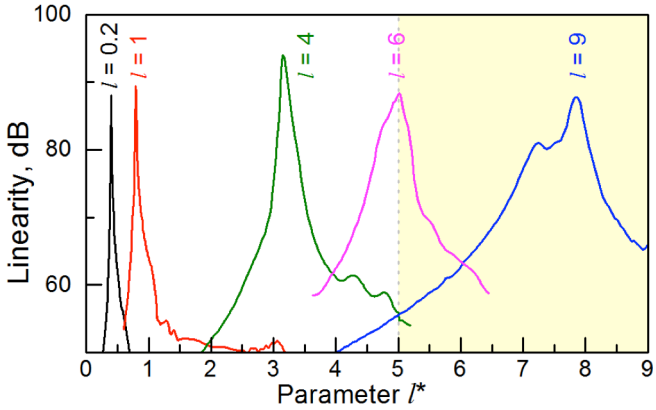

Fig. 6. The attainable linearity of bi-SQUID versus parameter $l^*=l\cdot i_{c3}$ at l = 0.2 (black line), 1 (red line), 4 (green line), 6 (magenta line), 9 (blue line). In the filled area (starting from $l^* \approx 5$) the flux-to-phase relation contains the more than 2 valued ranges increasing with l^*.

DOI: 10.1109/TASC.2016.2631427

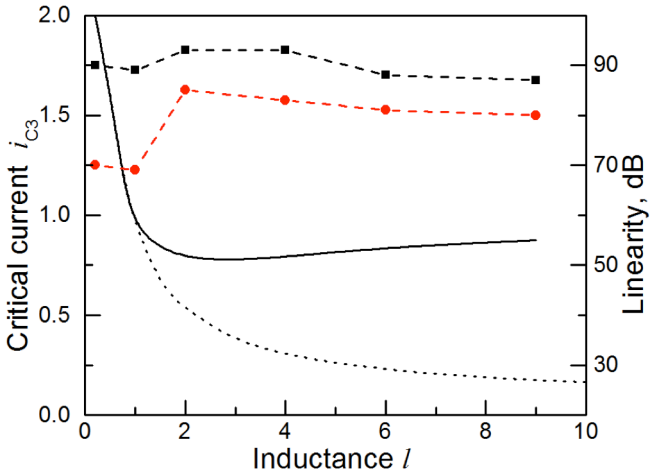

Fig. 7. The attainable linearity of the voltage output of bi-SQUID versus inductance l of the rf SQUID loop, when the signal exploits 30% (dash black line with squares) and 50% (dash red line with circles) of the total response swing, as well as the critical current i_{c3} conditioning the linearity (solid black line). For comparison, the dotted line replicates (from Fig. 4) i_{c3} answering triangular response form.

Fig. 6 shows the attainable linearity as a function of the parameter $l^* = l \cdot i_{c3}$ at different values of the rf SQUID loop inductance l = 0.2 (black line), 1 (red line), 4 (green line), and 9 (blue line). One can see that the commensurate high linearity can be achieved through either triangular voltage response with $l^* \sim 1$ at low inductances $l \leq 1$ or hysteretic response with $l^* > 1$ at higher inductances l. In the hysteretic mode, the two-valued response range ('a'-'a' range in Fig. 5, top) increases with l^* up to 0 to 2π range at $l^* \approx 5$, and then a more than two-valued part appears in the voltage response and increases with l^* (in the filled area in Fig. 6). When $l > 1$, the response linearity shows approximately the same dependence on departure of i_{c3} from its optimal value as shown for l = 1 in the inset in Fig. 4.

Fig. 7 summarizes the capabilities and conditions for the highly linear voltage output of bi-SQUID within wide range of the device inductance values l. Dash lines show the attainable linearity versus inductance l, when the signal exploits 30% (black line with squares) and 50% (red lines with circles) of the total response swing. Black solid line shows critical current i_{c3} conditioning the highest linearity. In hysteretic mode, the critical current is to be always of order of 1 (e.g., i_{c3} = 0.8 at l = 4 and i_{c3} = 0.87 at l = 9) that facilitates realization of such a device. For comparison, the dotted line replicates the substantially smaller critical current values of the third junction needed for approaching the triangular response.

V. Discussion

When realizing bi-SQUID, the inductance parameter l has to be chosen in compliance with tradeoff between the perfect linearity requirements, coupling ability, and transfer factor value. An increase of the one-junction loop inductance is desired for better coupling with an input circuit, but one should take into account the fact, that the transfer factor $\partial(V/V_c)/\partial\varphi_e$ decreases with inductance l as follows: it equals to ~ 0.63/π at l = 2, ~ 0.38/π at l = 4, and ~ 0.18/π at l = 9.

At the same time, the parameter l controls the extent of "multi-valuedness" of the voltage response. In compliance with the requirements for the perfect linearity, the operating point is to be specified by a dc flux (phase) biasing in the middle of the most linear part of the voltage response. If the operation conditions cannot secure against switching to the other branches of the multi-valued response (e.g., under random noise spikes), the operation point has to be set either on the single-valued part of the voltage response (outside the 'a'-'a' range in the response shown in Fig. 5, top) or at $\varphi_{ex} = \pi$ where both the response branches have the same linearity. In the first case, the two-valued range has to be reduced with the decrease in l^* to provide the middle point position of the most linear part of the voltage response on the single-valued part. In the second case, the two-valued range has to be increased with increase of l^* up to about 5 when the two-valued response ranges from 0 to 2π. However, the further increase of the inductive parameter has to be limited to approximately $l^* = 8$, since at higher values of l^* this work point ($\varphi_{ex} = \pi$) becomes related to the more than two-valued part of the voltage response.

VI. Conclusion

Our detail analysis confirms that bi-SQUID is capable of providing highly linear voltage output at very different values of the main (one-junction) loop inductance. Approximately the same high linearity (up to 90 dB) can be reached with a triangular-form response at $l \leq 1$ and hysteretic operation mode at $l > 1$. In all cases, the critical current of the third Josephson junction is to be of the same order as the one of the other two junctions. In addition, inductance l_{DC} of the two-junction loop is allowed to be as high as at least l/4 in the presence of the high linearity (for more details, see [20]). Both conditions are important for the realization of such high-linear circuit.

These results serve as a useful guidance in designing high-temperature superconductor bi-SQUIDs, as well as for achieving better coupling with an input circuit. Such circuits are important for a range of applications including linear low-noise amplifiers and high-sensitivity antennas [2]-[4], [21-22].

References

[1] V. K. Kornev, I. I. Soloviev, N. V. Klenov and O. A. Mukhanov, "Bi-SQUID - Novel Linearization Method for dc SQUID Voltage Response," *Superconductor Science and Technology*, vol. 22, 2009, p. 114011.

[2] G. V. Prokopenko , O. A. Mukhanov, D. E. A. Leese, Taylor B., M. C. De Andrade, S. Berggren , et al., "DC and RF measurements of serial bi-SQUID arrays," IEEE Trans. Appl. Supercond., vol. 23, p. 1400607, 2013.

DOI: 10.1109/TASC.2016.2631427

[3] S. Berggren, G. Prokopenko, P. Longhini, A. Palacios, et al., "Development of 2D Bi-SQUID arrays with high linearity," *IEEE Trans. Appl. Supercond*., vol. 23, no. 3, p. 1400208, Jun. 2013.

[4] M. C. de Andrade, A. Leese de Escobar, B. Taylor, S. Berggren, et al., "Detection of far field radio frequency signals by niobium superconducting quantum interference device arrays," *IEEE Trans. Appl. Supercond.*, vol. 25, no. 5, p. 1603005, 2015.

[5] P. Longhini, S. Berggren, Anna Leese de Escobar, A. Palacios, S. Rice, B. Taylor, et al., "Voltage response of non-uniform arrays of bi-superconductive quantum interference devices," *J. Appl. Phys*., vol. 111, p. 093920, 2012.

[6] Susan Berggren, Patrick Longhini, Anna Leese de Escobar, Antonio Palacios, Oleg Mukhanov, Georgy Prokopenko, "Modeling the effects of fabrication spreads and noise on series coupled arrays of bi-SQUIDs," *IEEE Trans. Applied Supercond.*, v. 26, No. 5, p. 1601205, 2013.

[7] Patrick Longhini, Susan Berggren, Antonio Palacios, Visarath In, Anna Leese de Escobar, "Coupled non-uniform bi-squid: A numerical investigation," Advances in Cryogenic Engineering: Transactions of the Cryogenic Engineering Conference-CEC, vol 1434, no. 57, pp. 1167-1174, 2013.

[8] Susan Berggren, Benjamin Taylor, Anna L De Escobar, "Modeling the Effects of Varying the Capacitance, Resistance, Temperature, and Frequency Dependence for HTS Josephson Junctions, DC SQUIDs and DC bi-SQUIDS," SPAWAR, San Diego CA, Tech. Rep. 2050, September 2014.

[9] Susan Berggren, Benjamin Taylor, Anna L de Escobar, Thomas Sheffield, Daniel Hallman, "Simulated bi-SQUID Arrays Performing Direction Finding," SPAWAR, San Diego CA, Tech. Rep. 2089, September 2015.

[10] S. Berggren, R. L. Fagaly, Anna Leese de Escobar, "Superconducting Quantum Interference Devices Arranged in Pyramid Shaped Arrays," *IEEE Trans. Applied Superconductivity*, vol. 25, no. 3, p. 1600605, 2015.

[11] S. Berggren, B.J. Taylor, E.E. Mitchell, K. Hannam, J.Y. Lazar, and Anna L. De Escobar, "Computational Modeling of bi-Superconducting Quantum Interference Devices (SQUIDs) for High Temperature Superconducting Prototype Chips," *IEEE Trans. Applied Supercond.*, v. 26, no. 5, 2016, p. 1601506.

[12] I. I. Soloviev, V. K. Kornev, N. V. Klenov, N. V. Kolotinskiy, "Design Issues of HTS bi-SQUID," *IEEE Trans. Applied Supercond.*, v. 26, no. 5, 2016, p. 1601205.

[13] A. Sharafiev, I. Soloviev, V. Kornev, M. Schmelz, R. Stolz, V. Zakosarenko, S. Anders, and H. Meyer, "Bi-squids with submicron cross-type josephson tunnel junctions," *Superconductor Science and Technology*, vol. 25, no. 4, pp. 45001–45005, 2012.

[14] S. A Cybart, E.Y. Cho, T.J. Wong, B. H. Wehlin, M. K. Ma, C. Huynh, R.C. Dynes, "Nano Josephson superconducting tunnel junctions in $YBa_2Cu_3O_{7-\delta}$ directly patterned with a focused helium ion beam," *Nature Nanotech*., vol. 10., no. pp.598-602, Jul. 2015.

[15] D. Drung and M. Mueck, The SQUID Handbook, vol. 1, ed. J. Clarke and A I Braginski, Weinheim: Wiley, 2004, pp 127–70.

[16] K. K. Likharev, Dynamics of Josephson junctions and circuits, New York: Gordon and Breach, 1986.

[17] V. K. Kornev, A. V. Sharafiev , I. I. Soloviev, O. A. Mukhanov, "Signal and noise characteristics of bi-SQUID," *Superconductor Science and Technology*, vol. 27, 2014, p. 115009.

[18] V. K. Kornev, A. V. Sharafiev , I. I. Soloviev, N. V. Kolotinskiy, V. A. Skripka, O. A. Mukhanov, "Superconducting Quantum Arrays," *IEEE Transactions on Applied Superconductivity*, vol. 24, No. 4, 2014, p. 1800606.

[19] Victor K Kornev , Nikolay V. Kolotinskiy , Vitaly A. Skripka , Alexey V. Sharafiev, Oleg A. Mukhanov, "Output power and loading of Superconducting Quantum Array," *IEEE Transactions on Applied Superconductivity*, v. 25, № 3, 2015, p. 1602005.

[20] V. K Kornev , N. V. Kolotinskiy , A. Yu. Levochkina, O. A. Mukhanov, "Critical current spread and thermal noise in bi-SQUID cells and arrays," *IEEE Transactions on Applied Superconductivity*, 2016, to be published.

[21] V. K. Kornev, I. I. Soloviev, A. V. Sharafiev, N. V. Klenov, O. A. Mukhanov, "Active electrically small antenna based on superconducting quantum array," *IEEE Trans. Appl. Supercond.*, vol. 23, no.3, p. 1800405, Jun. 2013.

[22] V. Kornev, I. I. Soloviev, N. V. Klenov, A. V. Sharafiev, and O. A. Mukhanov, "Array designs for active electrically small superconductive antennas," *Physica C*, vol. 479, pp. 119–122, Sep. 2012.